Catalysis Today 148 (2009) 119–123

Contents lists available at ScienceDirect

Catalysis Today

journal homepage: www.elsevier.com/locate/cattod

Photodegradation of 2,4-dichlorophenoxyacetic acid using ZnAlFe layered double hydroxides as photocatalysts

A. Mantilla [a], F. Tzompantzi [b,*], J.L. Fernández [a], J.A.I. Díaz Góngora [a], G. Mendoza [b], R. Gómez [b]

[a] CICATA-IPN, Av. Legaria No. 694, México 11500 D.F., Mexico
[b] Universidad Autónoma Metropolitana-Iztapalapa, Departamento de Química, Av. San Rafael Atlixco No. 186, México 09340 D.F., Mexico

ARTICLE INFO

Article history:
Available online 1 April 2009

Keywords:
ZnAlFe layered double hydroxides
LDHs co-precipitation
2,4-D adsorption
LDHs photocatalysts
2,4-Dichlorophenoxyacetic acid
LDHs memory effect

ABSTRACT

ZnAlFe layered double hydroxides (LDHs) with different Zn:Al:Fe ratio were obtained by the co-precipitation method and tested as photocatalysts for 2,4-dichlorophenoxyacetic acid (2,4-D) degradation. High specific surface areas (138–70 m^2/g) as well as semiconductor properties (band gap values of 2.59–2.00 eV) were obtained in the samples calcined at 673 K. When calcined samples were put in contact with as solution containing 300 ppm of 2,4-D, the reconstruction of the LDHs (memory effect) and an unexpected high capacity of 2,4-D adsorption were observed. The photodegradation in aqueous phase after saturation of the LDHs with 2,4-D showed that the confined (adsorbed) 2,4-D can be successfully degraded with ZnAlFe LDH photocatalysts.

© 2009 Elsevier B.V. All rights reserved.

1. Introduction

Dichlorophenoxyacetic acid (2,4-D), one of the most commonly used herbicides in controlling broadleaf weeds and other vegetation, is an aryloxyalkanoic acid; due to its polar nature, once absorbed it is translocated within the plant and accumulates at the growing points of roots and shoots where it inhibits growth. The 2,4-D residues are often reported in surface and ground water due to low soil sorption and high capacity for leaching [1]. 2,4-D is a well-known endocrine disrupter [2]; hence, treatment of such contaminants in water resources is inevitable. Photocatalysis, an advanced oxidation technology employing semiconductors as photocatalysts is a promising method for the elimination of organic pollutants like 2,4-D in water [3]. Among these materials we can mention TiO_2, ZnO, SnO_2 and more recently, layered double hydroxides (LDHs) [4].

LDHs belong to a class of anionic mineral clays, with structure of LDHs derived from mineral brucite, $Mg(OH)_2$. Brucite comprises a close packing of hydroxyl ions in which Mg^{+2} ions occupy alternative layers of octahedral sites, leading to stacking of charge-neutral metal hydroxide slabs of composition $[Mg(OH)_2]$. When a fraction of Mg^{+2} ions is isomorphously substituted by a trivalent ion such as Al^{+3} or Fe^{+3}, the positive charge generated on the metal hydroxide slab is compensated by the inclusion of anions generating the general formula $[M_{1-x}{}^{2+}\ M_x{}^{3+}\ (OH)_2]^{x+}\ (A^{n-})_{x/n}$: yH_2O, where M^{2+} and M^{3+} are divalent (Mg^{2+}, Fe^{2+}, Co^{2+}, Cu^{2+}, Ni^{2+}, Zn^{2+}) and trivalent (Al^{3+}, Cr^{3+}, In^{3+}, Mn^{3+}, Ga^{3+}, Fe^{3+}) metal ions, respectively and A^{n-} is an intercalate anion ($CO_3{}^{2-}$, $SO_4{}^{2-}$, NO^{3-}, F^-, Cl^-, being carbonate the most usual anion) [5–8]. By a controlled thermal decomposition, the LDHs are transformed into mixed oxides with homogeneous interdispersion of the elements, showing high specific surface areas among other interesting properties.

An increasing interest around the layered double hydroxides has been developing because of their multiple applications as basic catalysts [9], catalyst supports [10], adsorbents [11], anion exchangers [12], enzyme immobilizers [13] and medical oriented products [14] among others [15]. In addition to the previously mentioned applications, it has been recently reported that ZnAl LDHs can be used as successfull photocatalysts for the degradation of organic compounds, like methyl-orange [4], methylene blue [16] and phenol [17,18] in aqueous media. However, to our knowledge, ZnAlFe LDH materials have not been reported for this application.

With this in mind, in the present work the synthesis and characterization of ZnAlFe LDHs as well as their catalytic activity in the photodegradation of 2,4-D were studied. The characterization of the solids was done by X-ray diffraction (XRD), nitrogen adsorption and UV–vis spectroscopy and the photoactivity was evaluated in the photodegradation of the herbicide 2,4-dichlorophenoxyacetic acid. The selection of Zn and Fe instead of the traditional MgAl hydrotalcite was done because of the fact that ZnO [19] and Fe_2O_3 oxides [20,21] are well known for being photocatalytically active semiconductors.

* Corresponding author. Tel.: +52 55 58044669; fax: +52 55 58044666.
E-mail addresses: mmantillar0600@ipn.mx (A. Mantilla), fjtz@xanum.uam.mx (F. Tzompantzi).

0920-5861/$ – see front matter © 2009 Elsevier B.V. All rights reserved.
doi:10.1016/j.cattod.2009.02.036

2. Experimental

ZnAlFe double layered materials were prepared by the co-precipitation method by using aqueous solutions of $Zn(NO_3)_2{\cdot}6H_2O$, $Al(NO_3)_3{\cdot}9H_2O$ and $Fe(NO_3)_3{\cdot}9H_2O$ (J.T. Baker Analyzed Reagent) in the appropriate amounts to obtain 40 g of ZnAlFe with different molar ratios. The solutions containing the precursor compounds were added drop wise in a 1 L glass reactor vessel containing 800 mL of bidistilled water under vigorous magnetic stirring. After that, the pH of the solutions was adjusted to 9 by adding NH_2CONH_2 as precipitant agent. The resulting suspensions were vigorously stirred for 4 h at 363 K and maintained under reflux for 36 h. Then, the obtained materials were filtered and washed with deionized water. Before characterization, solids were dried at 373 K (dried samples) for 12 h and finally annealed at 673 K for 12 h in air flux 2 mL/s (calcined samples). The final composition of the samples was determined by atomic absorption technique, using an analyzer model S4 (Thermo Electron Corporation) and the obtained results are reported in Table 1. Samples were labeled as ZnAlFe-3, ZnAlFe-7 and ZnAlFe-10 for nominal Al^{3+}/Fe^{3+} ratios of 4.1, 1.85 and 1.0, respectively.

Specific surface areas were calculated by the BET method from the N_2 adsorption isotherms obtained with a Quantachrome Autosorb-3B equipment. X-ray analyses were obtained with a Siemens D500 X-ray diffractometer using a graphite crystal as monochromator to select Cu-Kα radiation (1.5406 Å) with a step of $0.02^\circ\ s^{-1}$. The band gap value was calculated from the absorption spectra obtained with a Cary 100 spectrophotometer equipped with an integration sphere. FTIR spectra were recorded in a PerkinElmer FT1730 spectrophotometer, using a nominal resolution of 4 cm^{-1} in order to improve the signal-to-noise ratio.

Prior to photocatalytic experiments, an adsorption study of 2,4-D on the annealed solids (673 K) was carried out by mixing the aqueous solution of 2,4-D (600 ppm) with the ZnAlFe synthesized LDH. The extent of equilibrium adsorption was determined from the decrease in 2,4-D concentration by UV–vis spectroscopy.

Photodegradation of 2,4-D was carried out in a glass batch reactor using 200 ml of a solution containing 300 ppm (1.35 mmol) of 2,4-D/g catalyst; a protected quartz tube with Pen-Ray power supply (UVP Products) with a typical λ of 254 nm and intensity of 4400 $\mu W/cm^2$ immersed in the solution was used as the source of irradiation. Before irradiation, the solution of 2,4-D and the catalyst were kept for 1 h without irradiation, until the complete adsorption of 2,4-D on the solid and then, the lamp was turned on. Three reactors were put simultaneously under irradiation for 1, 3 and 6 h respectively. After irradiation the solution was filtered and then the solid containing the residual 2,4-D previously adsorbed was analyzed. The evolution of 2,4-D at different time intervals was followed by FTIR spectroscopy analysis of the recovery LDH sample.

3. Results and discussion

3.1. Textural properties

Specific surface areas and ZnAlFe molar ratios and specific surface areas for prepared LDHs are reported in Table 1. It can be seen that specific surface areas diminish at lower Zn^{2+}/Al^{3+} molar ratios.

Table 1
Chemical composition, molar ratio and BET specific surface areas for the LDHs.

LDH	Chemical composition	Molar ratio $Zn^{2+}/Al^{3+} + Fe^{3+}$	Molar ratio Al^{3+}/Fe^{3+}	BET (m^2/g)
ZnAlFe3	$Zn_{1.99}Al_{2.04}Fe_{0.376}$	0.824	5.42	138
ZnAlFe7	$Zn_{1.27}Al_{0.90}Fe_{0.66}$	0.814	1.36	97
ZnAlFe10	$Zn_{1.99}Al_{0.802}Fe_{0.74}$	1.3	1.08	70

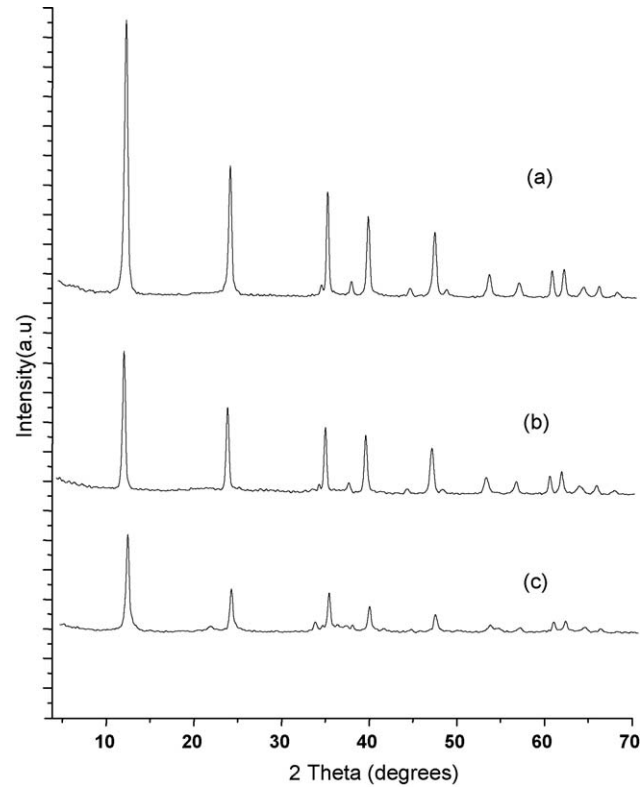

Fig. 1. X-ray diffraction patterns for LDHs: (a) ZnAlFe3, (b) ZnAlFe7 and (c) ZnAlFe10.

3.2. X-ray diffraction spectra

X-ray diffraction patterns obtained from the solids show a double layered hydroxide structure in all the samples (Fig. 1). The peak at 11.75 in 2θ angle, corresponding to the 0 0 3 reflection of the interlayer distance in the carbonated solid, can be clearly noted. The 0 0 3 reflection is typical of hydrotalcite-type materials and its intensity is related to the crystallinity degree of the material. If a hexagonal packing is assumed, the cell parameter can be calculated by means of the 0 0 3 and 1 1 0 reflection values using the equations $c = 3d_{003}$ and $a = 2d_{110}$, where c corresponds to three times the interlayer distance (0 0 3) and a is the average metal–metal distance in the interlayer structure (1 1 0).

The cell parameters show that the interlayer distance (d_{003}) was increased from 7.560 to 7.586 Å for the samples with the lowest and highest Fe^{3+} contents, respectively (Table 2). This variation in the cell parameter could be due to the different M^{2+}/M^{3+} ratios in the materials, since the increasing of the positive charge could provoke a higher repulsion between the layers of the materials. A high capacity for the adsorption of 2,4-D can be expected on theses samples, since the deficiency of the interlayer charges caused by the presence of Fe^{3+}, stabilizes the molecules with anionic properties.

3.3. Band gap energy

The evaluation of band gap energy (E_g) for the various samples was calculated using the Kubelka–Munk equation (Eq. (1)):

$$F(R) = \frac{(1-R)^2}{2R}, \quad (1)$$

Table 2
Cell parameters of the ZnAlFe LDH materials.

Catalyst	d_{003}	c parameter (Å)	a parameter (Å)
ZnAlFe3	7.5600	22.685	3.548
ZnAlFe7	7.5673	22.702	3.549
ZnAlFe10	7.5864	22.759	3.549

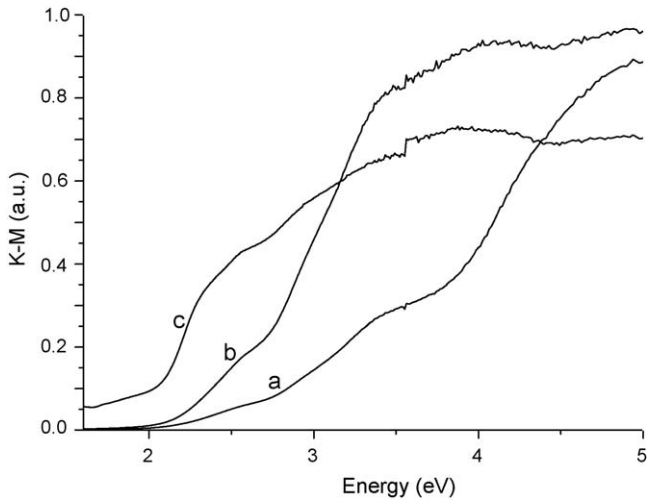

Fig. 2. UV–vis spectra of LDHs: (a) ZnAlFe3, (b) ZnAlFe7 and (c) ZnAlFe10.

where R is the reflectance (%) from the converted UV adsorption spectra (Fig. 2). The calculated E_g values are reported in Table 3, where it can be seen that E_g diminishes from 2.54 eV to 2.0 eV for the samples with the lowest and highest Fe^{3+} contents, respectively. These results show that Fe^{3+} in ZnAlFe LDH materials provokes important variations in the semiconductor properties of the solids.

3.4. Adsorptive and photocatalytic properties

The capacity of adsorption of 2,4-D in ZnAlFe LDHs materials was determined following a two-step procedure; in the first step, the calcined LDHs were placed in contact with several solutions at different concentrations of 2,4-D. The adsorption isotherms (Fig. 3) were obtained by the Langmuir linear equation (Eq. (2)) [22].

$$\frac{C_e}{Q} = \frac{C_e}{Q_m} + \frac{1}{K}, \quad (2)$$

where C_e is the concentration in the equilibrium in the liquid phase of the pesticide (mmol/L); Q is the quantity of 2,4-D (mmol) adsorbed in the equilibrium by gram of LDH; Q_m is the maximum amount adsorbed per unit mass of LDH (mmol/g) and K is the affinity constant (L/mmol). From the corresponding isotherms (Fig. 4), the calculated values (Table 3) show that the sample with the lowest Fe content (ZnAlFe3) presents the highest 2,4-D adsorption: 2.453 mmol (542 ppm) of 2,4-D/g cat; this value diminishes as the Fe^{3+} content increases in the material, being 1.946 mmol (430 ppm) and 1.676 mmol (370 ppm) of 2,4-D/g cat,

Table 3
2,4-D adsorbed amounts in the equilibrium on calcined LDHs, and time required for the 2,4-D photocatalytic degradation ($t_{1/2}$) using a UV light source.

LDHs	E_g (eV)	Q_m (mmol/g cat)	Q_m (2,4-D g/g cat)	$t_{1/2}$ (min)
ZnAlFe3	2.54	2.453	0.542	180
ZnAlFe7	2.48	1.946	0.430	150
ZnAlFe10	2.0	1.676	0.370	90

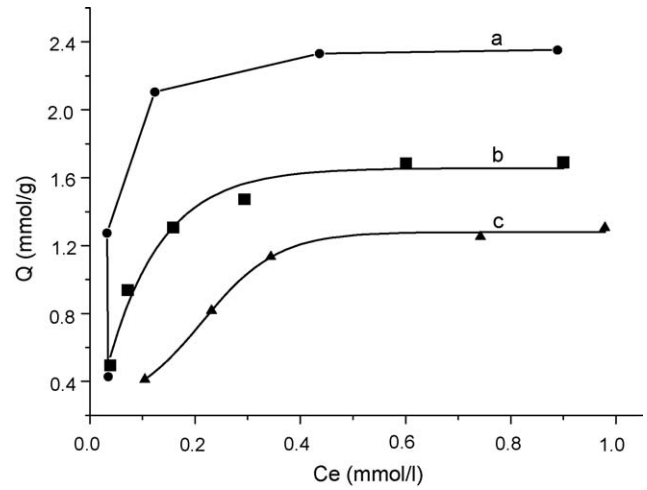

Fig. 3. Adsorption isotherms of 2,4-D on LDHs: (a) ZnAlFe3, (b) ZnAlFe7 and (c) ZnAlFe10.

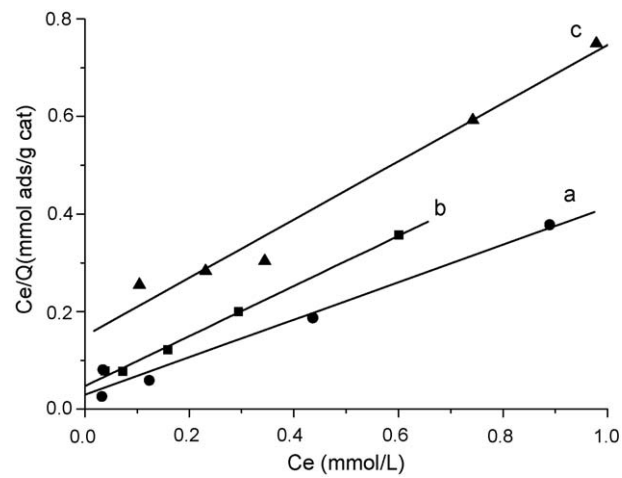

Fig. 4. Langmuir linear equation for 2,4-D adsorption on: (a) ZnAlFe3, (b) ZnAlFe7 and (c) ZnAlFe10.

for the ZnAlFe7 and ZnAlFe10 samples, respectively. As it can be expected, the decreasing in the sorption properties of ZnAlFe LDHs is correlated with the diminution in the specific surface area values.

During the adsorption experiments, the initial pH of the solution was 3; however, as the 2,4-D adsorption progressed the pH increases, reaching a value around 7.5 when the adsorption–desorption equilibrium was reached (Fig. 5). This variation in the pH strongly suggests a displacement of the OH surface by the 2,4-D anions.

LDHs materials can uptake anions from a solution by three different mechanisms: adsorption, intercalation by anion exchange and adsorption and intercalation by reconstruction of a calcined LDH. In the case of the present study, LDHs were calcined before the 2,4-D adsorption. X-ray diffraction patterns of the ZnAlFe3 LDH showed in Fig. 6 illustrate which of the mentioned adsorption mechanisms occurred in the ZnAlFe materials. In the figure, it can be seen the reconstruction of the sample, but the 0 0 3 reflection was strongly modified. A similar reconstruction and modification of the 0 0 3 reflection can be observed for ZnAlFe7 and ZnAlFe10 LDHs (Fig. 7). Anionic exchange was observed by Legrouri et al. [22] in the adsorption and exchange of 2,4-D on ZnAl hydrotalcites. They observed a 0 0 3 reflection at a 2θ value of 7.5, which corresponds to an interlayer distance of 1.9 nm in the ZnAl-2,4-D phase. The size calculated for the anions is 0.84 nm [11] and in ZnAlFe LDHs the

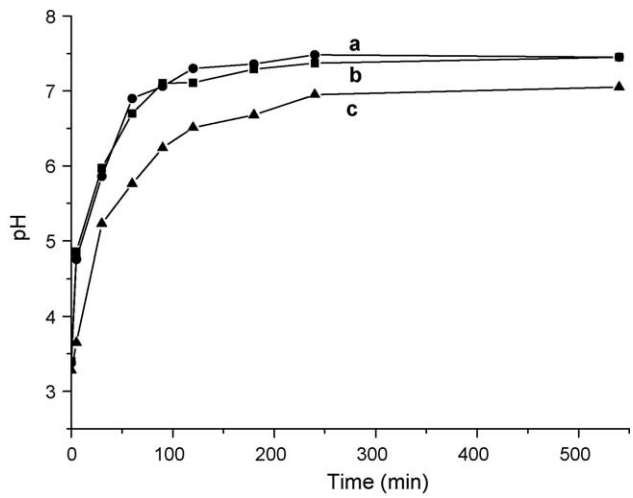

Fig. 5. Variation of the pH as a function of time for the ZnAlFe3 sample at various 2,4-D concentrations: (a) 100 ppm, (b) 200 ppm, and (c) 300 ppm.

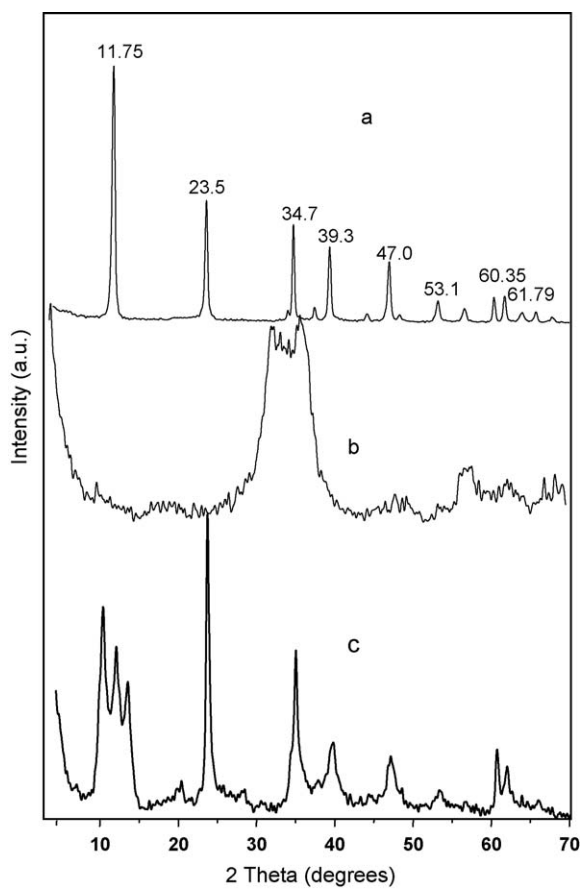

Fig. 6. X-ray diffraction patterns for the ZnAlFe3 sample: (a) dried, (b) calcined at 673 K, and (c) after 2,4-D adsorption on calcined sample.

interlayer distance is 0.75 nm for the 0 0 3 reflection, at 2θ value of 11.7. Thus, it can be assumed that the 2,4-D was preferentially adsorbed on the surface of the LDHs. The presence of the 0 0 3 reflections at 2θ value of 10.5 is not enough to justify the intercalation of the 2,4-D in the LDHs. The 2θ value at 10.5 could be due to the 0 0 3 reflection of some ZnAl LDH formed by a probable segregation in the solution containing the 2,4-D at pH 3.

The photolysis produced by the UV lamps in the solution containing 300 ppm of 2,4-D (blank test) was followed as a

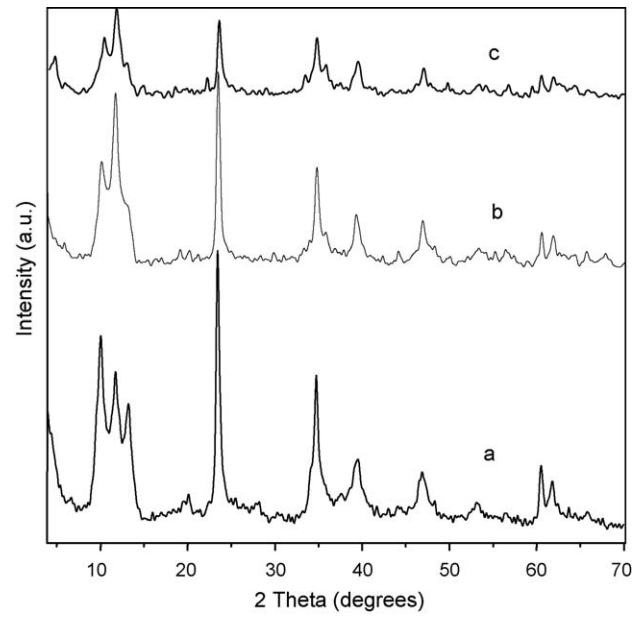

Fig. 7. X-ray diffraction patterns after 2,4-D adsorption on calcined samples: (a) ZnAlFe3, (b) ZnAlFe7, and (c) ZnAlFe10.

function of time and the results are reported in Fig. 8; it can be seen that the UV light source in absence of catalyst is not capable to degrade 2,4-D. Photodegradation study was carried out in samples where the saturation of the adsorbed 2,4-D was reached; the mechanism (on surface) by which the herbicide was adsorbed is not the purpose of the present work. In this way, LDHs were placed in contact with a solution containing 300 ppm of the pollutant for 1 h, since at such concentration, it is possible to assure that all the 2,4-D present in the solution is adsorbed after 1 h in contact with the LDHs. In Fig. 9, it can be seen that practically all the 2,4-D in the solution disappears after 1 h in contact with the solid.

Since the 2,4-D contained in the solution was totally adsorbed in the LDH material, the evolution of the 2,4-D degradation during the irradiation can only be followed by directly analyzing the disappearance of the adsorbed molecule as a function of time. According to the afore mentioned, the 2,4-D degradation as a function of time was estimated from the FTIR spectra, which were directly obtained from the solid following the C–O–C vibration band at $\sim$1290 cm^{-1} as it was reported by Legrouri et al. [22].

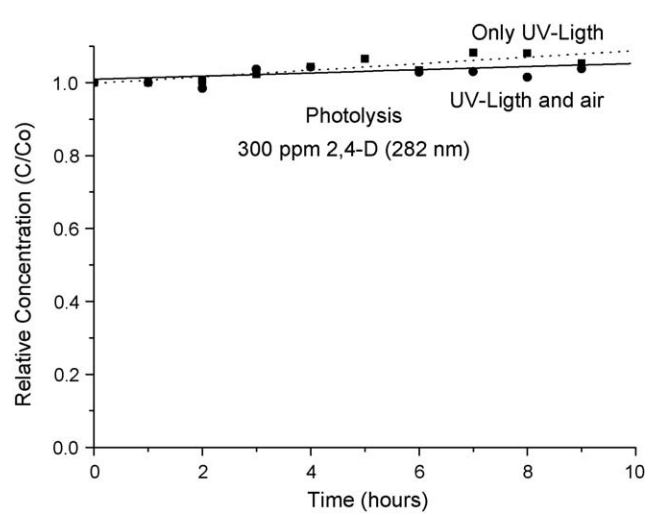

Fig. 8. Photodegradation (photolysis) of a solution containing 300 ppm of 2,4-D.

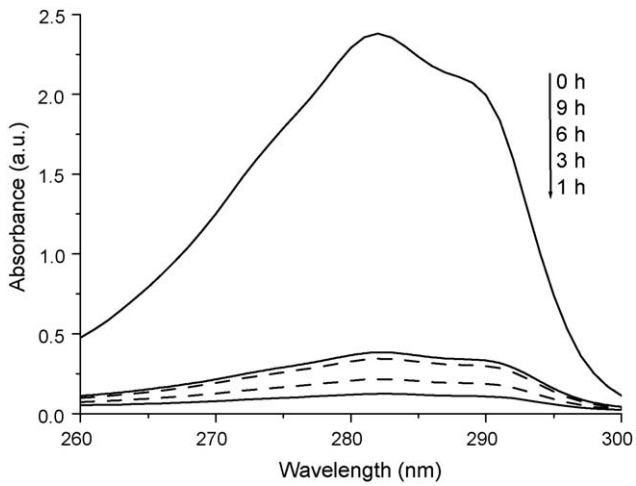

Fig. 9.

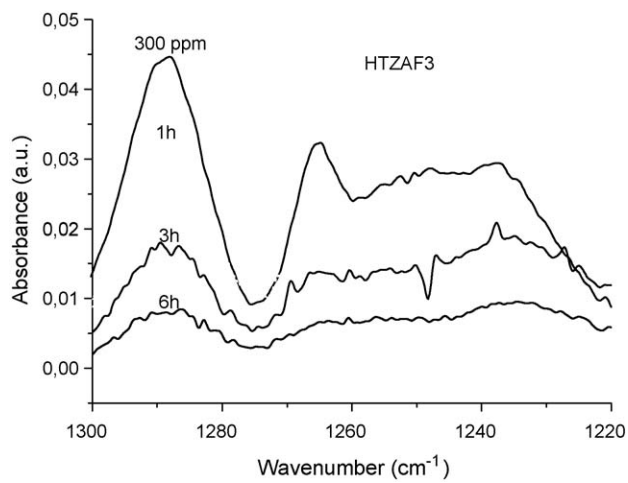

Fig. 10. UV absorption spectra of the 2,4-D solution as a function of time for the ZnAlFe3 calcined sample.

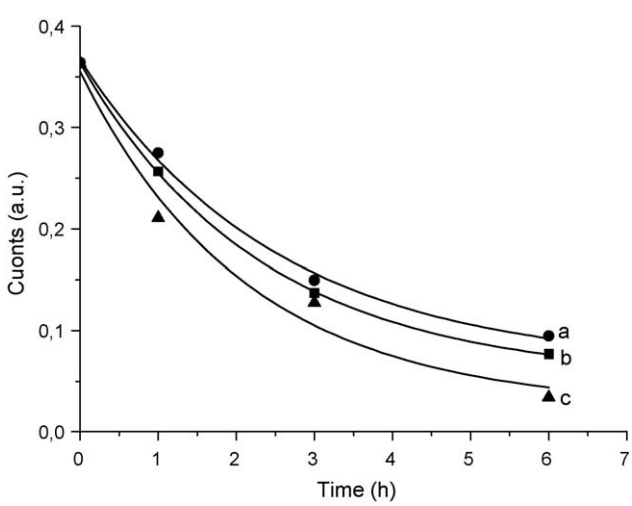

Fig. 11. FTIR spectra of the 1290 cm^{-1} vibration band as a function of time of irradiation for the ZnAlFe3 sample.

In order to illustrate the photocatalytic degradation process, the FTIR spectra of 2,4-D previously adsorbed on the solids as a function of time under irradiation for the ZnAlFe3 sample are shown in Fig. 10. The characteristic band of the C–O–C bond at ~1290 cm^{-1} can be seen in the spectra. To estimate the amount of 2,4-D decomposed as a function of time, the integrated values of the 1290 cm^{-1} band were used; the results are reported in Table 3 as $t_{1/2}$, which is the required time to discompose half of 2,4-D adsorbed in the LDHs. In Fig. 11, it can be seen that the photoactivity increases with the Fe^{3+} content. The high activity of the ZnAlFe10 solid is probably due to their lowest energy band gap and highest interlayer distance. These results show that 2,4-D can be stored in the solids and then destroyed by means of a photocatalytic process. In this photodegradation reaction, the ZnAlFe LDHs play the role of photocatalysts because of their semiconductor properties.

4. Conclusions

The results of the present work show that ZnAlFe materials can be synthesized from soluble salts, showing high specific surface area. LDH crystalline structure was obtained in all the synthesized samples. ZnAlFe LDH materials showed semiconductor properties with electron transitions at 644 nm (1.92 eV), 651 nm (1.90 eV) and 707 nm (1.75 eV) in the UV–vis region of the electromagnetic spectra. High adsorptive properties and high photodegradation activity of these materials for 2,4-D were evidenced. It is showed that the 2,4-D photodegradation can be successfully carried out with the solid totally saturated by adsorbed 2,4-D. These results showed that the pesticide can be confined on the LDHs and subsequently submitted to the photodegradation process.

Acknowledgments

We are indebted to SEP-CONACYT for the support provided to the CB-2006-1-62053 research project. A. Mantilla thanks CONACYT for scholarship support.

References

[1] J. Pichat, J.C. D_Oliveria, J.F. Maffre, D. Mas, Photocatalytic Purification and Treatment of Water and Air, Elsevier, Amsterdam, 1993, p. 683.
[2] T. Colborn, F.S. Vom Saal, A.M. Soto, Env. Imp. Ass. Rev. 14 (1993) 469.
[3] M.A. Fox, M.T. Dulay, Chem. Rev. (1993) 341.
[4] E.M. Seftel, E. Popovici, M. Mertens, K. De Witte, G. Van Tendeloo, P. Cool, E.F. Vansant, Micropor. Mesopor. Mater. 113 (2008) 296.
[5] A. Vaccari, Catal. Today 41 (1998) 53.
[6] F. Cavani, F. Trifiro, A. Vaccari, Catal. Today 11 (1991) 173.
[7] S. Miyata, Clays Clay Miner. 23 (1975) 369.
[8] A. De Roy, C. Forano, K. ElMalki, J.P. Besse, in: M.L. Occelli, H.E. Robson (Eds.), Synthesis of Microporous Materials, Expanded Clays and Other Microporous Systems, vol. 2, Van Nostrand Reinhold, New York, 1992 (Chapter 7).
[9] S. Abelló, F. Medina, D. Tichit, J. Pérez-Ramírez, J.E. Sueiras, P. Salagre, Y. Cesteros, Appl. Catal. B: Environ. 70 (2007) 577.
[10] F.-A. He, L.-M. Zhang, J. Coll. Interface Sci. 315 (2007) 439.
[11] L.P. Cardoso, J.B. Valim, J. Phys. Chem. Solids 67 (2006) 987.
[12] H. Goha, T.-T. Lima, Z. Dongb, Water Res. 42 (2008) 1343.
[13] S. Vial, V. Prevot, F. Leroux, C. Forano, Micropor. Mesopor. Mater. 107 (2008) 190.
[14] S.-J. Xia, Z.-M. Ni, Q. Xu, B.-X. Hu, J. Hu, J. Solid State Chem. 181 (2008) 2610.
[15] F. Melo, N. Morlanés, Catal. Today 133–135 (2008) 374.
[16] M. Parida, N. Baliarsingh, B. Sairam Patra, J. Das, J. Mol. Catal. A: Chem. 267 (2007) 202.
[17] R. Kun, M. Balázs, I. Dékány, Coll. Surf. A: Physicochem. Eng. Aspects 265 (2005) 155.
[18] A. Patzko, R. Kun, V. Hornok, I. Dekany, T. Engelhardt, N. Schall, Coll. Surf. A: Physicochem., Eng. Aspects 265 (2005) 64.
[19] S.K. Pardeshi, A.B. Patil, Sol. Energy 82 (2008) 700.
[20] R. Liou, S. Chen, M. Hung, C. Hsu, J. Lai, Chemosphere 59 (2005) 117.
[21] M. Noorjahan, V. Durga Kumari, M. Subrahmanyam, L. Panda, Appl. Catal. B: Environ. 57 (2005) 291.
[22] A. Legrouri, M. Lakraimi, A. Barroug, A. De Roy, J.P. Besse, Water Res. 39 (2005) 3441.